110 GHz Plasmonic Lithium Niobate Phase Modulator

Yilun Wang[1, †, *], Jihao Zhao[1, †], Xiaoyan Gao[1], Qiansheng Wang[2], Xi Xiao[2], Jian Cheng[1], Dingshan Gao[1], Wentao Gu[1], Wenchan Dong[1], Qizhi Yan[1], Liao Chen[1], Yu Yu[1], Chi Zhang[1], Xinliang Zhang[1, *]

1Wuhan National Laboratory for Optoelectronics and School of Optical and Electronic Information, Huazhong University of Science and Technology, Wuhan 430074, China

2National Information Optoelectronics Innovation Center, Wuhan 430074, China

*ylwang@hust.edu.cn, xlzhang@mail.hust.edu.cn

†These authors contributed equally to this work.

Abstract: An ultra-compact lithium niobate phase modulator based on the plasmonic slot waveguide is demonstrated with a length of ~16 µm, featuring a bandwidth exceeding 110 GHz and a high-rate operation beyond 90 Gbaud. © 2024 The Author(s)

1. Introduction

The terahertz (THz) wave band is considered the next frontier for meeting future data targets. With the growing demand for THz wireless applications, electro-optic modulators, as the core component for converting electrical signals into the optical domain, require a frequency response up to the THz range, high power handling, and low nonlinear distortion. Plasmonic polymer modulators [1], combining the ultra-small capacitance of the plasmonic slot waveguide (PSW) and the ultra-fast electro-optic effect of polymers, have realized bandwidth greater than 500 GHz [2] and have been applied to THz optical communication scenarios [3]. However, the process compatibility and temperature stability of electro-optic polymers require constant attention for commercial applications.

Due to the ultra-fast Pockels effect and the temperature stability, lithium niobate (LN) is widely used in current commercial electro-optic modulators. And the modulation efficiency has been greatly improved based on thin-film LN compared to the bulk LN [4]. Yet, the electrode spacing, the relative permittivity of LN, and the refractive index difference of LN waveguide affect the overlap coefficient between the optical field and the modulating electric field in LN, resulting in a modulation efficiency of ~2 Vcm and a length of millimeter dimension. The device size and complicated design of the traveling wave electrodes currently hinder thin-film LN modulators to a larger bandwidth of several hundred GHz and their further applications in THz optical communications.

In this work, we propose an ultra-compact high-speed LN phase modulator that combines the strong field confinement of PSW and the stability of LN film. The modulator is demonstrated with a 3-dB bandwidth exceeding 110 GHz and a C-band (1530-1565 nm) wavelength operation with low modulation depth variation. The data transmission with over 90 Gbaud binary phase shift keyed (BPSK) signals is carried out with a bit error ratio (BER) below 6.3×10^{-4}. Though the higher speed performance testing is limited by equipment, the present plasmonic LN modulator has shown great potential in high-speed optical communications and future THz optical communications.

2. Device design and fabrication

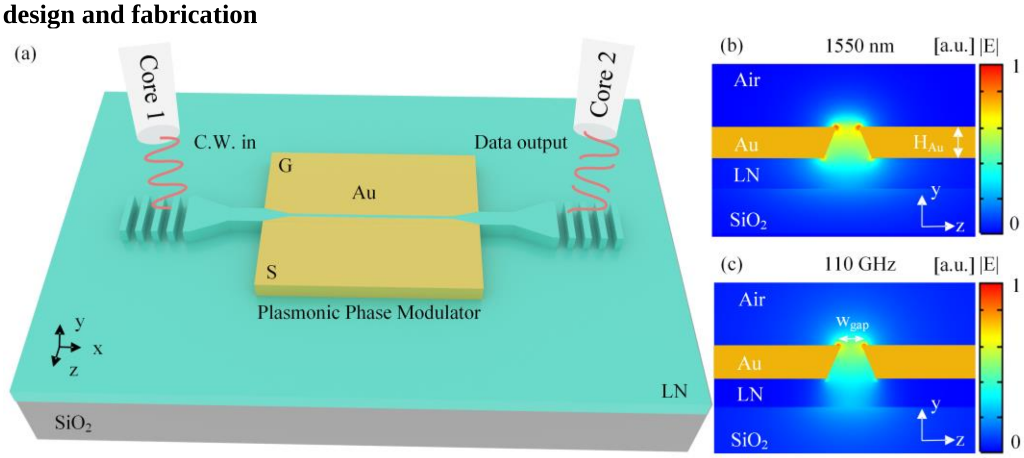

Fig. 1. (a) Schematic diagram of plasmonic LN phase modulator. (b), (c) Simulated mode profiles of the plasmonic field at 1550 nm (b) and the RF signal at 110 GHz (c).

Fig.1(a) shows the schematic of the designed plasmonic LN phase modulator. Two grating couplers (GCs) are utilized for in/out coupling to facilitate the test, and two 0.49-μm-long metal/LN tapers are used as photonic/plasmonic mode converters with a phase modulator section located between them. The continuous-wave (c.w.) infrared light is coupled through the GC and mode converter to the 15-μm-long metal/LN/metal waveguide, namely PSW. The phase of the plasmonic slot mode can be changed by applying modulating voltage on the electrodes owing to the Pockels effect of LN. As the limitations of the practical etching process, the LN waveguide sidewall has a 70-degree inclination. In practice, the ridge and GCs of LN are designed to the same depth to minimize process complexity, and the thickness of the gold electrodes grown on both sides is also the same as the ridge depth for optimal modulation. As shown in Figs. 1(b) and 1(c), the height of the electrode (H_{Au}) is 150 nm, and the upper width of the ridge (W_{gap}) is 140 nm. The small size of the plasmonic slot (LN ridge) makes the strong field constraints significantly enhance the interactions between the optical signals and the modulating radio frequency (RF) signals, resulting in efficient modulation. Meanwhile, the narrow spacing between two electrodes improves the electric field in the LN ridge, resulting in an obvious increase in modulation efficiency. In this structure, the LN modulator has a simulated modulation efficiency of 0.12 Vcm. The several microns length of the modulator decreases the RF losses and exhibits a capacitance of several fF. Thus, combined with the Pockels effect of LN, the proposed plasmonic LN phase modulator has the potential to achieve THz bandwidth.

The device was fabricated on a commercial LN-on-insulator sample with a top LN layer of 300 nm, a buried oxide layer of 4.7 μm, and a bottom Si layer of 525 μm. The GCs and LN ridge waveguides were patterned by electron beam lithography (EBL, Vistec EBPG 5000plus ES) and fabricated by inductively coupled plasma etching (Plasmalab system 100 ICP 180). Then, the two metallic electrodes were separately patterned by two EBLs and fabricated by e-beam evaporation (Ohmiker-50B), followed by two lift-off processes due to the narrow slot.

3. Device characteristics

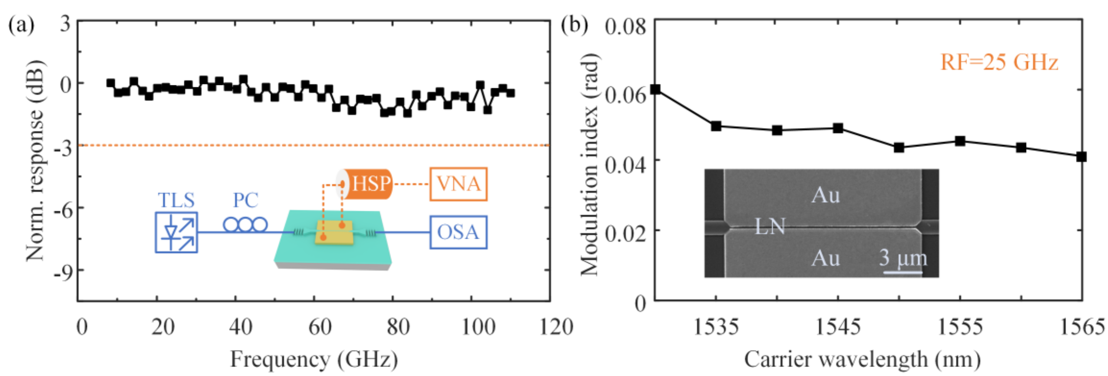

Fig. 2. (a) Measured frequency response as a function of the RF frequency. Inset: experimental set-up used to measure frequency response for various RF frequencies and carrier wavelengths. (b) Measured modulation index as a function of the carrier wavelength. Inset: the scanning electron microscope image of the phase modulator.

The inset of Fig. 2 shows the scanning electron microscope image of the phase modulator, demonstrating the close contact between the metal electrodes and the sidewall of the LN ridge. Thus, the surface plasmon polaritons can be effectively introduced on the metal/LN interface to confine the optical and RF fields. The detailed performances of the fabricated plasmonic LN phase modulator are measured as follows. The measured transmission losses of single grating couplers and PSW are 4.8 dB and 0.74 dB/μm, a little larger than the simulation results of 4.2 dB and 0.62 dB/μm due to the fabrication errors. The modulation bandwidth of the modulator is quantified by a 110 GHz vector network analyzer (VNA, keysight PNA N5227B) and an optical spectrum analyzer (OSA). Modulation efficiency is calculated by the power ratio of the first sideband and the carrier from the OSA. The inset of Fig. 2(a) shows the schematic of the bandwidth experimental set-up. An optical carrier in the C-band is provided by a tunable laser source (TLS) and controlled by the polarization controller (PC) for on-chip coupling. Then, the optical carrier is modulated by the electrical signal from the VNA through a high-speed probe (HSP) and coupled out to the OSA. The measured frequency response of the modulator up to 110 GHz is shown in Fig. 2(a). The modulator shows an ultra-flat response beyond 110 GHz, mainly due to the ultra-small capacitance and the fast response of the Pockels effect. To calculate the modulation depth variation for different carrier wavelengths, the phase modulation index for the C-band wavelength is measured with a sinuous signal frequency at 25 GHz and a driving voltage of V_p=1V. As shown in Fig. 2(b), the modulator achieves less than 1.7 dB modulation depth variation from 1530 nm to 1565 nm.

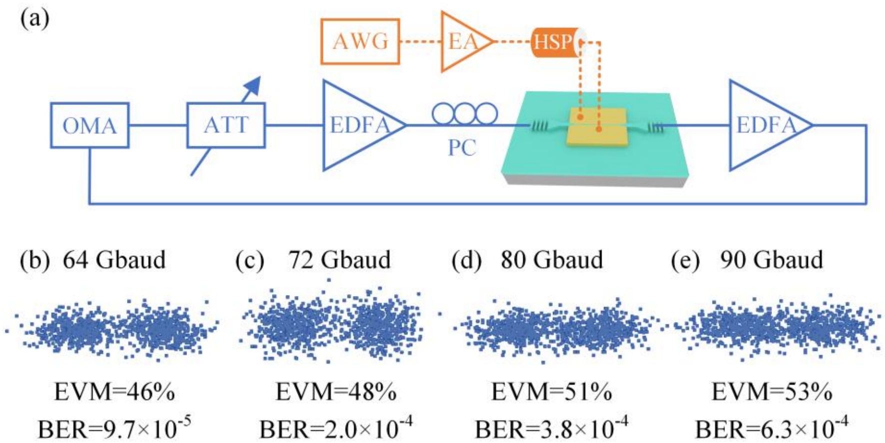

Fig. 3. (a) Experimental set-up for the transmission of BPSK signals. (b)-(e) Measured constellation diagrams, EVMs, and BERs of 64 Gbaud (b), 72 Gbaud (c), 80 Gbaud (d), and 90 Gbaud (e) BPSK signals

The following presents the high-data-rate signal transmission. Fig. 3(a) shows the schematic of the data transmission experiment. An optical carrier is provided by the optical modulation analyzer (OMA, keysight N4391B), attenuated by an attenuator (ATT) before being amplified by an erbium-doped fiber amplifier (EDFA), and controlled by the PC for on-chip coupling. Then, the optical carrier is modulated by the electrical signal, which is provided by the arbitrary waveform generator (AWG, keysight M8199A) and amplified by the electric amplifier (EA, GT-LNA-67 GHz). After that, the carrier is coupled out to another EDFA for signal amplification and sent back to the OMA. Combined with the local oscillating light provided by the OMA, the electrical signal encoded on the optical carrier can be coherently detected. To characterize the high-data-rate signal transmission, a data stream of a 2^7-1 long pseudo-random bit sequence (PRBS) is encoded on the proposed phase modulator with a rate up to 90 Gbaud. The actual electrical power loaded on the modulator is V_{pp} = 5 V, and the optical power entering the OMA is ~5 dBm. Figs. 4(b-e) shows the error vector magnitudes (EVMs) and BERs of 64 Gbaud, 72 Gbaud, 80 Gbaud, and 90 Gbaud BPSK signals obtained directly from the OMA. The BERs are below the hard-decision forward error correction (HD-FEC) limit, demonstrating a high-quality data signal modulation. Limited by the equipment, higher-data-rate signal transmissions are not carried out here. The combination of plasmonics and LN is a promising candidate for next-generation optical communications and future THz communications.

4. Summary

In this paper, the plasmonic LN phase modulator with a 3-dB bandwidth exceeding 110 GHz is experimentally demonstrated for the first time. Thanks to the PSW, the length of the LN phase modulator can be reduced to several microns, and the modulation efficiency can be increased to 0.12 Vcm. Moreover, based on the large-bandwidth plasmonic LN phase modulator, high-data transmission with rates up to 90 Gbaud for BPSK is successfully demonstrated with BERs below the HD-FEC limit. The plasmonic LN modulator shows potential for ultra-densely integrated high-speed optical communication systems.

5. Acknowledgements

The research is supported by the National Natural Science Foundation of China (Grant No. 61927817) and China Postdoctoral Science Foundation (BX20220123, 2022M720051).

6. References

[1] A.Melikyan, et al. "High-speed plasmonic phase modulators," Nat. Photonics **8**, 229–233 (2014).
[2] M. Burla, et al. "500 GHz plasmonic Mach-Zehnder modulator enabling sub-THz microwave photonics." APL Photonics **4**, 056106 (2019).
[3] S. Ummethala, et al. "THz-to-optical conversion in wireless communications using an ultra-broadband plasmonic modulator." Nat. Photonics **13**, 519–524 (2019).
[4] C. Wang, et al. "Integrated lithium niobate electro-optic modulators operating at CMOS-compatible voltages," Nature **562**, 101-104 (2018).